Observation of quantum beating in a simple beam-splitting experiment: Two-particle entanglement in spin and space-time

Y. H. Shih and A. V. Sergienko
Department of Physics, University of Maryland, Baltimore County, Baltimore, Maryland 21228
(Received 29 September 1993)

A single light beam, generated by type-II down-conversion, is split by a beam splitter. When a set of quartz plates is inserted into the single beam, the coincidence counting rate between the split beams exhibits a 100% frequency-beating modulation. This nonclassical phenomena is a manifestation of a two-photon entangled state in which the two-particle state is entangled simultaneously in spin and space-time.

PACS number(s): 42.50.Dv, 42.50.Wm, 03.65.Bz

Two-particle entangled states have been known since the early days of quantum mechanics. These states play a particularly important role in the study of the Einstein-Podolsky-Rosen (EPR) paradox [1] and in the test of Bell's inequalities [2]. It was Schrödinger who first pointed out that a particular type of two-particle state, which he called an "entangled state," is responsible for the EPR paradox [3]. Entangled states are states of two or more particles that cannot be written as products of single-particle states. An example of a two-particle entangled state was given in EPR's 1935 paper where the measurement of an observable of either particle determined the value of that observable for the other particle with unit probability [1]. Although the two-particle entangled EPR states are predicted by quantum theory, they are not allowed in classical physics. The physical consequences resulting from the EPR states violate classical local realism [4].

Two-particle entanglement has been demonstrated by two types of experiments in the past: (1) two-particle polarization correlation measurements; most of the historical EPR-Bohm experiments [5] and Bell's inequality measurements exhibited nonlocal two-particle polarization entanglement [6-11]. (2) Two-particle interference (fourth-order interference) experiments; recent two-particle nonclassical interference experiments demonstrated the two-particle space-time entanglement [12–26]. A typical two-particle polarization entanglement fringe is a sine function of coincidence counting rate between spatially separated detection events against the relative orientation of the independent polarization analyzers. A typical two-particle space-time entanglement fringe is an interference pattern of coincidence counting rate between the spatially separated detection events against the optical path difference between two beams, which usually involves ordinary interferometer(s). In contrast to the nonlocal coincidence counting rate, each of the single detector counting rates in these experiments remains constant when the polarizer orientation or the optical path difference is manipulated. It has been understood that two types of two-particle entangled states are responsible for the above two types of nonclassical interference phenomena: (1) spin entanglement and (2) space-time entanglement [4].

We wish to report an experiment which shows another type of two-particle entanglement: (3) spin and space-time entanglement. The spin and space-time combined nonlocal interference phenomena exhibits quite unusual behavior in comparison with previous experiments. For example, in the following reported experiment, a pair of orthogonally polarized light quanta with different colors is injected collinearly through a single port of a beam-splitter and detected by two independent photon counting detectors placed in the two output ports of the beam splitter with two linear polarization analyzers and narrow bandwidth spectral filters. The bandwidths of the filters are narrow enough so that each of the detectors picks up only one color. There is no preferred polarization orientation in each of the three (incident, transmitted, and reflected) beams. There is no single detector counting rate change when the orientation of the polarization analyzers or the optical path difference between the orthogonally polarized components is manipulated. There is not even a coincidence counting rate change when manipulating the optical path difference without having polarizers in each of the transmitted and reflected beams. However, a beating fringe with 100% modulation shows up in the coincidence counting rate by inserting crystal quartz plates in the incident beam with the help of correctly orientated polarizers in each of the transmitted and reflected beams. It is this spin and space-time entangled state (simultaneously) which makes it possible to demonstrate two-particle nonlocal interference in a simple beam-splitting experiment.

The schematic experimental setup is illustrated in Fig. 1. A cw argon ion laser line of 351.1 nm is used to pump an 8 mm $\times$8 mm $\times(0.56\pm0.05)$-mm BBO (β-BaB_2O_4) nonlinear crystal. The BBO is cut at a type-II phase-matching angle to generate a pair of orthogonally polarized signal and idler photons collinearly around 702-nm wavelengths. The down-converted beam is separated from the pumping beam by a UV grade fused silica dispersion prism, then directed collinearly at a near normal incident angle to a polarization independent beam splitter which has 50% - 50% reflection and transmission coefficients. A single photon detector is placed in each transmission and reflection output ports of the beam splitter. The photon detectors are dry ice cooled

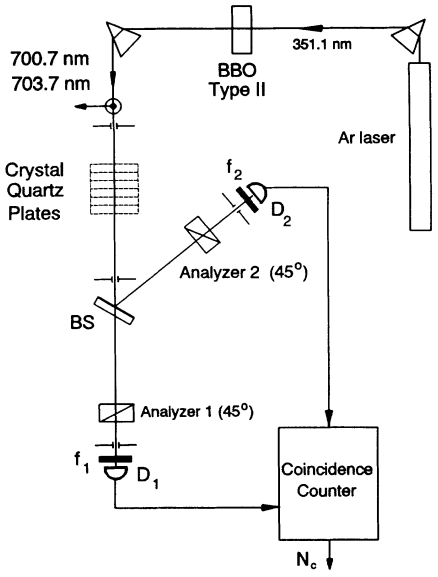

FIG. 1. Schematic experimental setup. BS denotes a beam splitter, f is a filter, D is a photon detector, and BBO is a β-$Ba_zB_2O_4$ crystal.

avalanche photodiodes operated in photon counting Geiger mode. A Glan-Thompson linear polarization analyzer, followed by a narrow bandwidth interference spectral filter, is placed in front of each of the detectors. The polarization analyzers are oriented at 45° to the ordinary-ray (o-ray) polarization planes of the BBO crystal. The spectral filters f_1 and f_2 have Gaussian shape transmission functions centered at conjugate wavelengths of the down-conversion, $\lambda_1=700.7$ nm and $\lambda_2=703.7$ nm, respectively. The spectral bandwidths are both 1 nm in full width at half maximum. Practically, there is no frequency overlap between the two filters. The output pulses of the detectors are then sent to a coincidence circuit with a 3-nsec coincidence time window. The two detectors are separated by about 2 m; compared to the coincidence time window the detection events are spatially separated events.

A set of 15 crystal quartz plates is placed in the incident beam for changing the optical path difference, Δl, between the orthogonally polarized signal and idler photons. The fast axes of the quartz plates were carefully aligned to match the o-ray or e-ray polarization planes of the BBO crystal during the measurements. Each of the quartz plates is (1.0 ± 0.1) mm in thickness, resulting in an optical path difference $(n_e-n_o)L\cong 9$ μm between the o-ray and e-ray. The 15 quartz plates were aligned carefully one by one before the taking of data, and moved away one by one during the measurements. Two sets of measurements were made in order to have 31 experimental points to show the modulation of the interference. In the first (second) set, we aligned the fast axes of the quartz plates to match the o-ray (e-ray) polarization plane of the BBO. The two-photon coincidence counting rate was observed to show a frequency beating fringe when the polarization analyzers were oriented at 45°,

$$R_c\cong R_0[1-\cos(2\pi/\lambda_1-2\pi/\lambda_2)(\Delta l)]\ , \tag{1}$$

where λ_i is the center wavelength of the ith spectral filter, and Δl is the optical path difference introduced by the quartz plates.

Figure 2 reports typical observed two-photon coincidence rate measurements as a function of Δl. The coincidence counts are direct measurements, with no "accidental" subtractions or any other theoretical corrections. Each of the data points corresponds to a different number of quartz plates remaining in the incident beam. The left (right) side's 15 points, which are indicated by a "$-$" sign ("$+$" sign), of data were taken under the following condition: the fast axes of the quartz plates coincide with the o-ray (e-ray) polarization plane of the BBO crystal. It is clear that the interference pattern has a period of about 164 μm, which corresponds to the beating frequency 1.83×10^{12} Hz, of the down-converted beams. The modulation visibility is $(97\pm2)\%$.

Contrary to the coincidence counting rate, the single detector counting rates do not show any modulations, as is reported in the upper part of Fig. 2.

To explain these measurements theoretically, we present a simple quantum mechanical model. According to the standard theory of type-II parametric down-conversion, the two-photon state can be written as [17]

$$|\Psi\rangle=\int d\omega_p\, A(\omega_p)\int d\omega_1 d\omega_2\,\delta(\omega_1+\omega_2-\omega_p)\times a_o^\dagger(\omega_1)a_e^\dagger(\omega_2)|0\rangle\ , \tag{2}$$

where ω represents the frequencies for signal (1), idler (2), and pump (p) of the down conversion. The δ function represents perfect frequency phase matching of the down conversion, i.e., $\omega_1+\omega_2=\omega_p$. The wave number phase matching condition $\mathbf{k}_1+\mathbf{k}_2=\mathbf{k}_p$ is implicit in the choice of the locations of the pinholes which direct the down-converted beams to the detectors; in this experiment we consider collinear down-conversion. The subscript indices o and e for the creation operators indicate the ordinary and extraordinary rays of the down conversion, traveling along the same direction as the pump, the z direction. The defined x and y coordinate axes coincide with the o-ray and e-ray polarization directions of the crystal. A (ω_p) is a spectral distribution function for the laser line, which is usually considered to be a Gaussian. Different from type-I down-conversion, the two-photon state is entangled in polarization, frequency, and wave number (vector). It is not difficult to see from state (2) that for each pair of the conjugate frequency components ω_1 and ω_2, the state is entangled in polarization:

$$[a_o^\dagger(\omega_1)a_e^\dagger(\omega_2)+a_e^\dagger(\omega_1)a_o^\dagger(\omega_2)]|0\rangle\ .$$

The fields at the detectors 1 and 2 are given by

$$\begin{aligned}E_1^{(+)}(t)&=\alpha_t\int d\omega\, f(\omega)[\exp(-i\omega t_1^o)\hat{\mathbf{e}}_1\cdot\hat{\mathbf{e}}_o a_o(\omega)\\&\quad+\exp(-i\omega t_1^e)\hat{\mathbf{e}}_1\cdot\hat{\mathbf{e}}_e a_e(\omega)]\ ,\\E_2^{(+)}(t)&=\alpha_r\int d\omega\, f(\omega)[\exp(-i\omega t_2^o)\hat{\mathbf{e}}_2\cdot\hat{\mathbf{e}}_o a_o(\omega)\\&\quad+\exp(-i\omega t_2^e)\hat{\mathbf{e}}_2\cdot\hat{\mathbf{e}}_e a_e(\omega)]\ ,\end{aligned} \tag{3}$$

where $\hat{\mathbf{e}}_i$ is in the direction of the ith linear polarization

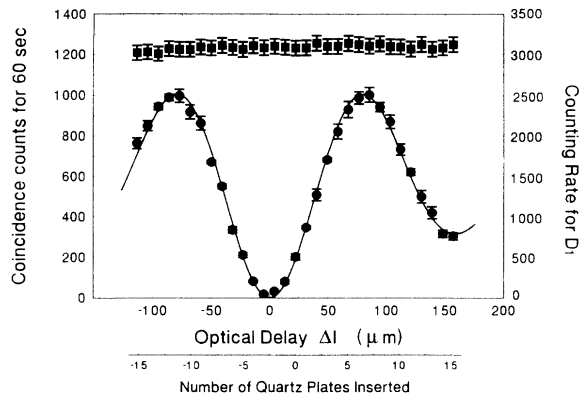

FIG. 2. Lower curve: Coincidence counts in 60 sec as a function of Δl, which corresponds to a certain number of quartz plates. The solid curve is a fitting curve of Eq. (7). The modulation visibility is (97±2)% (no accidental subtractions). Upper curve: Single detector counting rate (per second) as a function of Δl.

analyzer axis, $a_o(\omega)$ and $a_e(\omega)$ are the destruction operators for the o-ray and e-ray, α_t and α_r are the complex transmission and reflection coefficients of the beam splitter, and $f(\omega)$ is the spectral transmission function of the filters. The t_i's are given by $t_i^o = t - l_i^o/c$, $t_i^e = t - 1_i^e/c$, $i=1$ and 2, where $l_i^{o,e} = \int dz\, n^{o,e}(z)$ indicates the optical path for the o-ray or e-ray of the ith beam, with $n^{o,e}(z)$ being the refractive index at position z. We have approximated $(dn/d\omega)_o - (dn/d\omega)_e \cong 0$ for simplifying the calculation. The use of pinholes, which limit the transverse width of the beams, allows a good one-dimensional approximation. The coincidence counting rate is

$$R_c = (1/T)\int\int_0^T dT_1 dT_2 \langle \Psi | E_1^{(-)} E_2^{(-)} E_2^{(+)} E_1^{(+)} | \Psi \rangle \times S(\tau, \Delta T_c) = (1/T)\int\int_0^T dT_1 dT_2 |\Psi(t_1,t_2)|^2 S(\tau, \Delta T_c) , \quad (4)$$

where $\tau \equiv T_1 - T_2$, T_i is the detection time of the ith detector, $S(\tau, \Delta T_c)$ is a function that describes the coincidence circuit, and ΔT_c is the time window of the coincidence circuit. For $\tau > \Delta T$, $S(\tau, \Delta T_c) \cong 0$, and for $\tau < \Delta T$, $S(\tau, \Delta T_c) \cong 1$. If the coincidence time window is large enough, S can be considered as one at time t. The time integral can be taken to infinity as a good approximation. In Eq. (4), an effective two-photon wave function $\Psi(t_1,t_2)$, which is realized by the coincidence measurement at the two detectors, is defined by

$$\Psi(t_1,t_2) = \langle 0 | E_1^{(+)}(t_1) E_2^{(+)}(t_2) | \Psi \rangle . \quad (5)$$

The introduction of $\Psi(t_1,t_2)$ is helpful for the understanding of physics.

It is straightforward to show from (2), (3), and (5) that

$$\Psi(t_1,t_2) = \alpha_t \alpha_r [\hat{\mathbf{e}}_1 \cdot \hat{\mathbf{e}}_o \hat{\mathbf{e}}_2 \cdot \hat{\mathbf{e}}_e A(t_1^o, t_2^e) + \hat{\mathbf{e}}_1 \cdot \hat{\mathbf{e}}_e \hat{\mathbf{e}}_2 \cdot \hat{\mathbf{e}}_o A(t_1^e, t_2^o)] , \quad (6)$$

where $A(t_1,t_2)$ is calculated in the Appendix. The two terms in (6) correspond to two probability amplitudes: (1) *o-ray transmitted ⊗ e-ray reflected* and (2) *e-ray transmitted ⊗ o-ray reflected.* The effective wave function (6) indicates two-particle entanglement in both spin and space-time.

Substituting $A(t_1,t_2)$ [Appendix Eq. (A5)] into Eq. (6), the coincidence counting rate is calculated as

$$R_c = R_{c0}[1 - \exp(-\sigma\delta/2)\cos(\Omega_1 - \Omega_2)\delta] , \quad (7)$$

where $\delta \equiv \Delta l/c$ is the optical delay between the o-ray and the e-ray, and Ω_i is the ith filter's center frequency. The 45° orientation of the analyzers has been taken into account. We use a right-handed natural coordinate system with respect to the **k** vector as the positive z-axis direction. Care has to be taken to follow the rules of the natural coordinate system, especially for the reflected beam.

Equation (7) indicates an interference beating of the coincidence counting rate at frequency $\Omega_1 - \Omega_2$ with 100% modulation when Δl is near zero. The modulation visibility vanishes exponentially when Δl is off from zero. The solid curve in Fig. 2 is a fitting curve of Eq. (7).

It is interesting to see that the zero point of the counting rate is not in the case of zero quartz plates. The reason is that the refractive indices for the o-ray and e-ray of the BBO crystal also contribute to the optical delay δ, $\delta = \delta_{\text{BBO}} + \delta_{\text{quartz}}$. BBO is a negative uniaxial crystal and quartz is a positive uniaxial crystal. If we align the BBO and the quartz plates in such a way that the o-ray polarization plane of BBO and the e-ray polarization plane of quartz plates coincide, the optical delay inside the BBO can be compensated for by the quartz plate for a certain value of thickness. From repeated measurements, we conclude that the zero point of the coincidence counting rate happens at a point in which about $2.4 \times (1.0 \pm 0.1)$-mm quartz plates are placed in the beam path. The difference of refractive indices $(n_e - n_0)$ of quartz is about 0.009 around 700 nm. $c/u_o - c/u_e \cong (n_o - n_e)$ of BBO at this phase matching angle for 702.2 nm is about 0.077, where $u_{o,e}$ are the group velocities for the o-ray and e-ray, respectively. It indicates that 2.4 mm of quartz plate will compensate for about half of the thickness of the 0.56-mm BBO crystal which was used in the measurements. This effect suggests that the average "birth place" of the twin brother photon pair is in the middle of the down-conversion crystal, which is reasonable. Mathematically, this compensation effect is to make a complete overlap of the spatial part of the two-photon effective wave function $A(t_1^o, t_2^e)$ and $A(t_1^e, t_2^o)$ in Eq. (6).

The above quantum beating phenomenon demonstrated a two-photon entangled state in spin and in space-time generated by type-II spontaneous parametric down-conversion. The simultaneous double entanglement may easily be seen from the following argument: neither the transmitted nor the reflected beam has a preferred polarization or a preferred optical path (short or long path in the quartz plates); however, if the photon in the transmitted beam is measured to be polarized at θ_1, the photon in

the reflected beam must have been polarized at $\theta_1=\theta_2$. At the same time, if the photon which triggered detector 1 is the one which took a shorter path in the quartz, the one which triggered detector 2 must have been the one which took a longer path, and vice versa. The measurement of the observables of either particle (spin and space-time) determines the value of these observables for the other particle with unit probability. The (97±2)% visibility coincidence interference pattern is the signature of this particular double entanglement.

We wish to thank M. H. Rubin, D. N. Klyshko, and M. A. Horne for many helpful discussions. We are grateful for the assistance of data taking by T. B. Pittman. This work was supported by the Office of Naval Research Grant No. N00014-91-J-1430.

APPENDIX

From (2), (3) and (5),

$$A(t_1,t_2)=\int d\omega_p\, A(\omega_p)\int\int d\omega_1 d\omega_2 f_1(\omega_1)f_2\omega_2)\delta(\omega_1+\omega_2-\omega_p)\exp(-i\omega_1 t_1)\exp(-i\omega_2 t_2)\ , \tag{A1}$$

where $t_j=t-l_j/c$, $j=1$ and 2, $l_j=\int dz\, n(z)$, and n is the refractive index. Assuming Gaussian spectrum distributions with equal widths σ for both signal and idler,

$$f_j(\omega_j)=f_0\exp\left[-\frac{(\omega_j-\Omega_j)^2}{2\sigma^2}\right]\ ,\quad j=1,2\ . \tag{A2}$$

Substituting into (A1) and making the change of variables $\nu_+=\nu_1+\nu_2$ and $\nu_-=(\nu_1-\nu_2)/2$ gives

$$A(t_1,t_2)=\int d\omega_p\, A(\omega_p)\exp\left[-i\frac{\Omega_p(t_1+t_2)}{2}\right]\exp\left[-i\frac{\Omega_d(t_1-t_2)}{2}\right]$$
$$\times\int d\nu_+\int d\nu_- f_0^2\exp\left[-\frac{\nu_+^2}{4\sigma^2}\right]\exp\left[-\frac{\nu_-^2}{\sigma^2}\right]\exp\left[-i\frac{\nu_+(t_1+t_2)}{2}\right]\exp(-i\nu_-(t_1-t_2))\delta(\nu_+-\Delta\omega_p)\ , \tag{A3}$$

where $\Delta\omega_p=\omega_p-\Omega_p$ and $\Omega_d=(\Omega_1-\Omega_2)/2$. The integral (A3) over ν_+ is easily done using the δ function. In doing the integral over ν we use the fact that Ω_1 and Ω_2 are both much greater than σ to extend the integral from $-\infty$ to $+\infty$. This is just a Gaussian integral which leads to the result

$$A(t_1,t_2)=u(t_1-t_2)v(t_1+t_2)\ ,$$
$$u(t)=\exp\left[-\frac{\sigma^2t^2}{4}\right]\exp\left[-i\frac{\Omega_d t}{2}\right]\ , \tag{A4}$$
$$v(t)=\exp\left[-i\frac{\Omega_p t}{2}\right]\int d\omega_p\, A(\omega_p)\exp\left[-i\frac{\Delta\omega_p t}{2}\right]\exp\left[-\frac{\Delta\omega_p^2}{4\sigma^2}\right]\ ,$$

where all constants have been incorporated into $A(\omega_p)$. For a Gaussian spectrum and narrow bandwidth of $A(\omega_p)$, $(\Delta\omega_p\ll\sigma)$, (A4) can be approximated:

$$A(t_1,t_2)=A_0\exp\left[-\frac{\sigma_p^2(t_1+t_2)^2}{8}\right]\exp\left[-\frac{\sigma^2(t_1-t_2)^2}{4}\right]\exp\left[-i\frac{\Omega_1 t_1}{2}\right]\exp\left[-i\frac{\Omega_2 t_2}{2}\right]\ . \tag{A5}$$

[1] A. Einstein, B. Podolsky, and N. Rosen, Phys. Rev. **47**, 777 (1935).
[2] J. S. Bell, Physics **1**, 195 (1964).
[3] E. Schrödinger, Naturwissenschaften **23**, 807 (1935); **23**, 823 (1935); **23**, 844 (1935). A translation of these papers appears in *Quantum Theory and Measurement,* edited by J. A. Wheeler and W. H. Zurek (Princeton University Press, Princeton, 1983).
[4] M. A. Horne, A. Shimony, and A. Zeilinger, Phys. Rev. Lett. **62**, 2209 (1989).
[5] D. Bohm, *Quantum Theory* (Prentice-Hall, Englewood Cliffs, NJ, 1951).
[6] For a review, see J. F. Clauser and A. Shimony, Rep. Prog. Phys. **41**, 1881 (1976).
[7] A. Aspect, P. Grangier, and G. Roger, Phys. Rev. Lett. **47**, 460 (1981).

[8] Y. H. Shih and C. O. Alley, Phys. Rev. Lett. **61**, 2921 (1988).
[9] Z. Y. Ou and L. Mandel, Phys. Rev. Lett. **61**, 50 (1988).
[10] P. G. Kwiat, A. M. Steinberg, and R. Y. Chiao, Phys. Rev. A **45**, 7729 (1992).
[11] T. E. Kiess, Y. H. Shih, A. V. Sergienko, and C. O. Alley, Phys. Rev. Lett. **71**, 3893 (1993).
[12] Z. Y. Ou and L. Mandel, Phys. Rev. Lett. **61**, 54 (1988).
[13] J. D. Franson, Phys. Rev. Lett. **62**, 2205 (1989).
[14] P. G. Kwiat, A. M. Steinberg, and R. Y. Chiao, Phys. Rev. A **47**, 2472 (1993).
[15] J. Brendel, E. Mohler, and W. Martienssen, Phys. Rev. Lett. **66**, 1142 (1991).
[16] T. S. Larchuk, R. A. Campos, J. G. Rarity, P. R. Tapster, E. Jakeman, B. E. A. Saleh, and M. C. Teich, Phys. Rev. Lett. **70**, 1603 (1993).
[17] D. N. Klyshko, *Photons and Nonlinear Optics* (Gordon and Breach, New York, 1988).

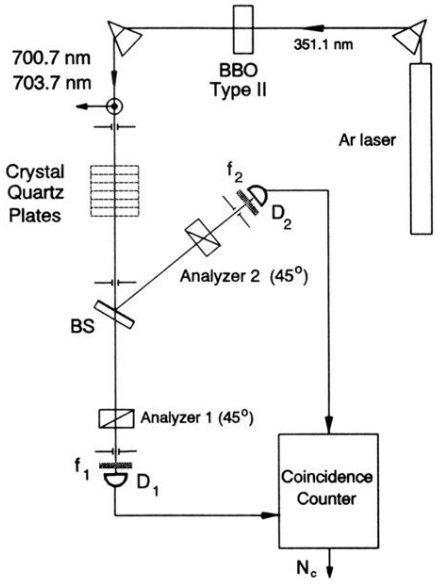

FIG. 1. Schematic experimental setup. BS denotes a beam splitter, f is a filter, D is a photon detector, and BBO is a β-$Ba_zB_2O_4$ crystal.